



# Grain boundary wetting of different types of grain boundaries in the Cu–Ag system

Ivan Mazilkin<sup>a,b,\*</sup>, Kristina Tsoy<sup>b</sup>, Alexander Straumal<sup>b</sup>, Alexey Rodin<sup>c</sup>, Brigitte Baretzky<sup>a</sup>

<sup>a</sup> Karlsruhe Institute of Technology, Institute of Nanotechnology, Hermann-von-Helmholtz-Platz 1, 76344 Eggenstein-Leopoldshafen, Germany

<sup>b</sup> Institute of Solid State Physics RAS, Ac. Ossipyan str. 2, 142432 Chernogolovka, Russia

<sup>c</sup> National University for Science and Technology "MISIS", Leninsky prospect 4, 119049 Moscow, Russia



## ARTICLE INFO

### Article history:

Received 16 March 2020

Accepted 27 March 2020

Available online 27 March 2020

### Keywords:

Grain boundaries

Wetting phase transition

Copper

CSL grain boundaries

Grain boundary character distribution

EBSD

## ABSTRACT

Present work is dedicated to the investigation of grain boundary (GB) wetting phase transition on different types of grain boundaries in the Cu–Ag system. The character of GBs in the samples was determined by the electron backscattering diffraction. GB character distribution was based on the coincidence site lattice (CSL) model and on the values of the misorientation angle of GBs. Experimental results show that only the low angle GBs and the  $\Sigma 3$  CSL GBs do not reach complete wetting by the melt. Random high misorientation angle (HA) GBs reach complete wetting at 895 °C. Only  $\Sigma 11$ ,  $\Sigma 5$  and  $\Sigma 13$  CSL GBs have a higher wetting temperature than the HA GBs, so their GB energy should be lower than the energy of HA GBs.

© 2020 Elsevier B.V. All rights reserved.

## 1. Introduction

The wetting phenomenon is known for many centuries. If a droplet of a liquid is placed on the solid surface, in some cases it will spread over the whole available surface of the solid. This effect is based on the balance of surface tension energies and on the tendency of any system to lower its free enthalpy. If wetting occurs, then, by spreading the liquid, the system substitutes a highly energetic solid/gas interface with a layer of liquid and two interfaces: solid/liquid and liquid/gas ones. Recently it became clear that this phenomenon can be considered as a surface phase transition. Cahn [1] and Ebner [2], who theoretically proved this concept, predicted that the wetting effect could also be found on internal boundaries in materials with two or more phases. Later these theoretical assumptions were proven right by experimental investigations on individual grain boundaries (GBs) [3,4] and polycrystals [5–8].

Recently a new investigation method has been developed that made it possible to get deeper into the wetting phenomenon of GBs. The electron backscattering diffraction (EBSD) method [9] gave the opportunity to differentiate between different GB types and investigate the wetting transition not as a spectrum of wetting temperatures, but as a spectrum of different GBs with different

wetting temperatures. The present work expands the previous results [10] to a new level of understanding the GB wetting.

## 2. Material and methods

The Cu–10 wt% Ag alloy was obtained from high purity components (5N8 Cu and 5N6 Ag) by vacuum induction melting and casting into rods of  $\varnothing 10$  mm. Disks 1 mm thick were cut from these ingots and sealed in evacuated quartz ampoules with a residual pressure of approximately  $4 \times 10^{-4}$  Pa at room temperature. The Cu–Ag samples were annealed at 785, 790, 795, 815, 835, 875, 895, 915, 975 and  $1015 \pm 2$  °C. Samples were annealed for 2 h and then quenched in water with ampoules. The temperatures, composition, and annealing time were chosen based on previous work [10] in such a way that the equilibrium fraction of the liquid in the system was between 0 and 0.15. The examined area of the Cu–Ag phase diagram is given in Fig. 1.

After quenching, the samples were sealed in an electrically conductive resin. Then, they were mechanically ground and polished using, at the last stage of polishing, a  $\text{SiO}_2$  suspension with a grain size of 0.05  $\mu\text{m}$  and an automatic vibration polisher. Polished samples were examined using a LEO 1530 VP scanning electron microscope (SEM) equipped with a system for measuring EBSD and a backscatter detector (BSD). The BSD detector was used to make micrographs with a very high resolution of the same parts of the structure that were measured by the EBSD method. This was done

\* Corresponding author at: Institute of Solid State Physics RAS, Ac. Ossipyan str. 2, 142432 Chernogolovka, Russia

E-mail address: [mograine@yandex.ru](mailto:mograine@yandex.ru) (I. Mazilkin).

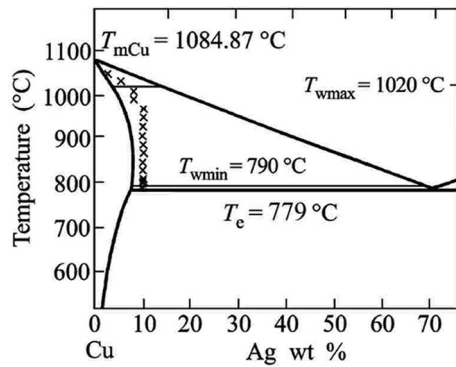


Fig. 1. The Cu-Ag equilibrium phase diagram [11]. The small crosses mark experimental points.

to ensure that GB wetting layers thinner than 1  $\mu\text{m}$  would be found. The EBSD method was used in a standard setup: working distance 12 mm, voltage 25 kV. The scans were  $1000 \times 1000$  point big, collected with a 1  $\mu\text{m}$  step size. A “Copper” structure file was modified by substituting atoms of copper by silver, according to the experimental concentration.

### 3. Theory

Wetting of GBs differs from the wetting of a free surface. The main difference is that in case of wetting of a free surface the effect is controlled by the equilibrium of three surface energies at the sitting droplet. In case of GB wetting by the liquid phase, only two types of surface energies take part in the equilibrium, namely the GB energy  $\sigma_{GB}$  and the energy of solid/liquid interphase boundary  $\sigma_{SL}$ . When a GB is incompletely wetted by a liquid, the two solid/liquid interfaces form a contact angle  $\theta$ . The dependence between the surface energies and the contact angle can be described by the Young’s formula modified for the GB wetting:

$$2\sigma_{SL} = \sigma_{GB} \cos \frac{\theta}{2}$$

In case of investigating the GB wetting in a polycrystal by analyzing the 2D section of a 3D structure, the analysis of contact angle values can’t be applied, because there is no information how the observed GBs are inclined under the visible surface of the sample section. If a GB is completely covered by the second phase from one triple joint to another, then the GB is considered as completely wetted. All other GB morphology cases are considered as incompletely wetted.

In the present work, all data sets were processed on the OIM TSL software. First, the confidence index (CI) of the scan was evaluated. If the CI was bigger than 0.5 (min value 0, max value 1) it meant that there are enough data points, which are very close to the structure file that was used to index the measurement. In this case further basic cleaning operations were performed, such as CI standardization, neighbor CI correlation and partitioning of points with a CI value lower than 0.1. Fig. 2 shows a typical orientation map of a structure after all cleaning procedures. After that the GBs on the orientation map were evaluated for wetting, simultaneously compared to the BSD micrograph to ensure exact evaluation.

The results were collected into wetting data sets, the GBs were divided into chosen GB types and in each GB type the fractions of wetted GBs were calculated for each annealing temperature. From previous work we know that the temperature dependences of the fractions have an asymptotic form tending to 1. Based on this assumption, an exponential asymptotic function was fitted to every set of points. The Origin software was used to fit the functions. Using the fitted functions the wetting temperatures

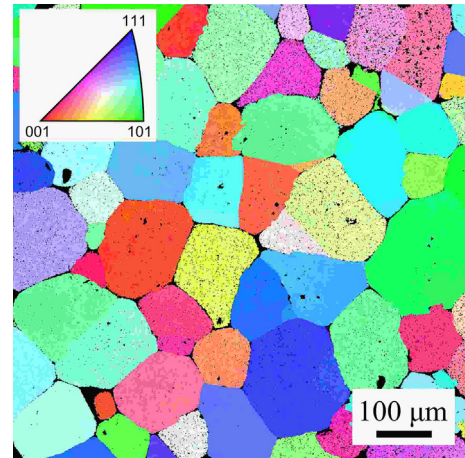


Fig. 2. The Cu-Ag sample microstructure in the form of the IPF color coded map.

were derived. The GB types were respected completely wetted when function were reaching saturation and the fraction of wetted GBs was higher than 0.95.

### 4. Results and discussion

First wetted random high misorientation angle (HA) GBs were found at 790  $^{\circ}\text{C}$ . This confirms the previous results [10]. Some of the resulting temperature dependences of the fraction of the wetted GBs are given in Fig. 3. It can be clearly seen that the CSL  $\Sigma 3$  GB do not reach complete wetting. The low misorientation angle GBs (not pictured in Fig. 3) do not reach complete wetting either.

The contributions of these two GB types to the “All GB” line results in a saturation level of about 0.95. The data points for the GB misorientation angle and the CSL  $\Sigma 13$  GBs show a typical shape of the temperature dependences for GBs that reach complete wetting. Wetting temperatures of different GB types derived from data sets are presented in Table 1. The wetting results for the GB types in the Cu-Ag systems differ from those of the Cu-In results [12]. Clearly, the HA GBs have a much broader wetting temperature range than in Cu-In alloys, and the minimal wetting temperature is not equal to the peritectic temperature, but is 10 to 15  $^{\circ}\text{C}$  higher. The CSL  $\Sigma 5$  GBs have a higher wetting temperature than the HA GBs. This can be the result of a different deviations spectrum of

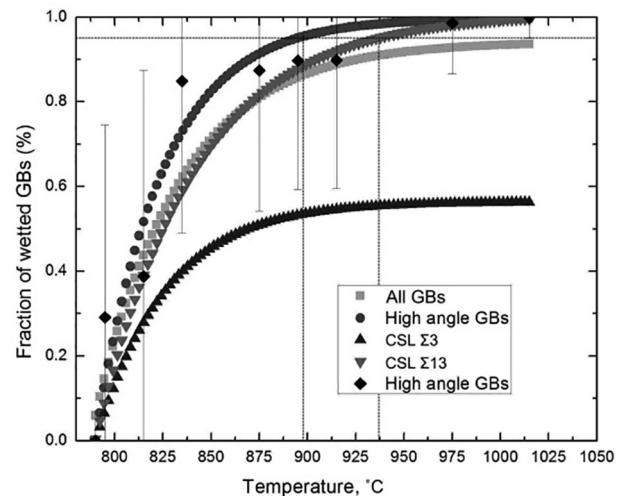


Fig. 3. Temperature dependence of the fraction of wetted GBs for different GB types.

**Table 1**  
GB wetting temperatures for different GB types.

GB type	$T_{\text{wetting}}$
CSL $\Sigma 23$	831 °C
CSL $\Sigma 7$	832 °C
CSL $\Sigma 15$	860 °C
CSL $\Sigma 9$	865 °C
CSL $\Sigma 17$	880 °C
High angle GBs	895 °C
CSL $\Sigma 11$	908 °C
CSL $\Sigma 5$	930 °C
CSL $\Sigma 13$	937 °C
Low angle GBs	Don't reach complete wetting
CSL $\Sigma 3$	Don't reach complete wetting

$\Sigma 5$  GBs from the ideal  $\Sigma 5$  structure. The analysis of the deviation distributions and GBs attribution criterion to the CSL GBs may explain the differences. If those parameters for both systems are equal, than we could conclude, that the difference in the second element affects the structure of the  $\Sigma 5$  GBs and changes their surface energy. Further extensive analysis and comparison is required.

## 5. Conclusions

By increasing temperature, first GBs are wetted at 790 °C. Low misorientation angle GBs and the CSL  $\Sigma 3$  GBs show the most special wetting behavior and don't get completely wetted in the present temperature range. The CSL  $\Sigma 5$ ,  $\Sigma 11$  and  $\Sigma 13$  GBs show special behavior too. They become wetted at temperatures higher than 895 °C. 895 °C is the wetting temperature of the HA GBs. Other CSL GBs are wetted at lower temperatures.

## Declaration of Competing Interest

The authors declare that they have no known competing financial interests or personal relationships that could have appeared to influence the work reported in this paper.

## Acknowledgement

The authors acknowledge the financial support of the Russian foundation for basic research (Grant 18-33-00473).

## References

- [1] J.W. Cahn, Critical-point wetting, *J. Chem. Phys.* 66 (1977) 3667, <https://doi.org/10.1063/1.434402>.
- [2] C. Ebner, W. Saam, New phase-transition phenomena in thin argon films, *Phys. Rev. Lett.* 38 (1977) 1486–1489, <https://doi.org/10.1103/PhysRevLett.38.1486>.
- [3] B.B. Straumal, S.A. Polyakov, E.J. Mittemeijer, Temperature influence on the faceting of Sigma 3 and Sigma 9 grain boundaries in Cu, *Acta Mater.* 54 (2006) 167–172, <https://doi.org/10.1016/j.actamat.2005.08.037>.
- [4] J. Schölhammer, B. Baretzky, W. Gust, E. Mittemeijer, B. Straumal, Grain boundary grooving as an indicator of grain boundary phase transformations, *Interface Sci.* 9 (2001) 43–53, <https://doi.org/10.1023/A:1011266729152>.
- [5] R.M. German, P. Suri, S.J. Park, Review: liquid phase sintering, *J. Mater. Sci.* 44 (2009) 1–39, <https://doi.org/10.1007/s10853-008-3008-0>.
- [6] D. Ross, D. Bonn, J. Meunier, Observation of short-range critical wetting, *Nature* 400 (1999) 737–739, <https://doi.org/10.1038/23425>.
- [7] D. Laporte, E. Watson, Experimental and theoretical constraints on the melt distribution in crystal sources – the effect of crystalline anisotropy on the melt interconnectivity, *Chem. Geol.* 124 (1995) 161–184, [https://doi.org/10.1016/0009-2541\(95\)00052-N](https://doi.org/10.1016/0009-2541(95)00052-N).
- [8] B. Straumal, W. Gust, T. Watanabe, Tie lines of the grain boundary wetting phase transition in the Zn-rich part of the Zn-Sn phase diagram, *MSF* 294–296 (1999) 411–414, <https://doi.org/10.4028/www.scientific.net/MSF.294-296.411>.
- [9] N. Brodusch, H. Demers, R. Gauvin, Imaging with a commercial electron backscatter diffraction (EBSD) camera in a scanning electron microscope: a review, *J. Imag.* 4 (2018) 88, <https://doi.org/10.3390/jimaging4070088>.
- [10] A.B. Straumal, B.S. Bokstein, A.L. Petelin, B.B. Straumal, B. Baretzky, A.O. Rodin, A.N. Nekrasov, Apparently complete grain boundary wetting in Cu-In alloys, *J. Mater. Sci.* 47 (2012) 8336–8343, <https://doi.org/10.1007/s10853-012-6773-8>.
- [11] T.B. Massalski, *Binary Alloy Phase Diagrams*, ASM International, Materials Park, OH, 1990.
- [12] A.B. Straumal, V.A. Yardley, B.B. Straumal, A.O. Rodin, Influence of the grain boundary character on the temperature of transition to complete wetting in the Cu-In system, *J. Mater. Sci.* 50 (2015) 4762–4771, <https://doi.org/10.1007/s10853-015-9025-x>.